RESEARCH ARTICLE
doi: 10.2306/scienceasia1513-1874.2022.046

ScienceAsia 48 (2022): **202–208**

In-situ synthesis of sodium doped g-C_3N_4 by high temperature copolymerization and photocatalytic performance

Ni Bai[a], Jiahui Yin[a], Xiaoxia Huo[b], Yajun Ma[a], Dandan Guo[a], Aimin Wang[a,*]

[a] Shaanxi Key Laboratory of Low Metamorphic Coal Clean Utilization, School Chemistry and Chemical Engineering, Yulin University, Yulin 71900 China

[b] College of Chemistry and Chemical Engineering, Xi'an University of Science and Technology, Xi'an 710054 China

*Corresponding author, e-mail: aimin_wang@yulinu.edu.cn

Received 1 Jun 2021
Accepted 1 Dec 2021

ABSTRACT: Na^+-doped g-C_3N_4 (Na(x)-CN) was synthesized via a facile *in-situ* thermal polymerization with dicyandiamide and sodium chloride and compared with g-C_3N_4 treated with sodium chloride solution (CN/NaCl) and g-C_3N_4 combined with sodium chloride (CN@NaCl). The resultant catalysts were characterized by various analytical methods. The results showed that Na^+ was doped into the lattice gap of g-C_3N_4 by forming Na-N bond, which improved the valence band energy level of the catalyst and enhanced the oxidizability of holes (h^+). In addition, the introduction of Na^+ inhibited the growth of g-C_3N_4 grains, increased the specific surface area of g-C_3N_4 and the adsorption of dissolved oxygen and pollutants in water, which significantly improved the photocatalytic performance. The visible light catalytic performance of the catalyst gradually improved with the increase of Na^+-doped content. The Na(0.1)-CN (sodium loading was 1.36%) showed the best photocatalytic performance, and the degradation rate was about 10 times that of g-C_3N_4. The degradation rate of MB reached 87% after 4 h of illumination.

KEYWORDS: sodium ion, carbon nitride, Na-doped graphite-carbon nitride, visible light, photocatalysis

INTRODUCTION

With the rapid development in renewable energy, the energy conversion and storage systems are becoming increasingly important [1]. Graphite phase carbon nitride (g-C_3N_4) is a 2D lamellar semiconductor similar to graphene, which has the characteristics of easy preparation, stability, non-toxicity, no pollution, visible light response, etc. Therefore, it has received extensive attention from researchers in the environmental field [2, 3]. However, g-C_3N_4 prepared by traditional methods often has the problems of small specific surface area, narrow visible light response range and high recombination rate of photogenerated electron-hole pairs [4]. Therefore, many researchers are committed to the modification of photocatalysts such as morphology control [5–7], doped modification [8–10] and heterostructure formation with other substances [11–13].

Transition metal element-doped introduces impurity energy levels, reduces band gap and increases the specific surface area and extends the light absorption range of g-C_3N_4 [14]. For example, doping Fe [15], Ti [16], Zn [17], W [18], Cu [19], Mo [20], etc. can generate new acceptor energy levels below the conduction band or above the valence band of g-C_3N_4, thereby improving its photocatalytic activity. The chemical properties of alkali metal elements are generally active, so they are often used to adjust the electronic structure of photocatalysts [21]. Mohammad et al [22] prepared Na,O-co-doped g-C_3N_4 by thermal copolymerization of urea and sodium hydroxide. It was found that Na,O-g-C_3N_4 has a low detection limit and high sensitivity for the electrochemical detection of hydrogen peroxide. Li et al [23] used thiourea and potassium iodide to synthesize K^+-doped g-C_3N_4 photocatalyst by thermal polymerization. The results showed that K^+ and N form K-N bond, adjust the band gap position of g-C_3N_4, reduce the band gap width, broaden the light response range and visible light absorption capacity, increase the separation efficiency of photo-generated carriers, and thus enhance the oxidation capacity of photo-generated holes. Guo et al [24] used dicyandiamide and potassium iodide as raw materials to prepare K and I co-doped g-C_3N_4 by thermal polymerization. It was found that K-doped mainly increased the electron migration rate, while I-doped enhanced the response to visible light. Jiang et al [25] dispersed g-C_3N_4 in MOH (M refers to Li, Na or K) solution to prepare alkali metal doped g-C_3N_4. The results showed that alkali metal doping increases the specific surface area of g-C_3N_4, reduces the band gap and improves the electronic structure of effective charge transfer.

In this work, Na^+-doped g-C_3N_4 photocatalyst was prepared *in-situ* by high-temperature copolymerization method by taking dicyandiamide and sodium chloride as raw materials, and its structure and morphology were characterized, and the synthesis mechanism of Na^+-doped g-C_3N_4 and the photocatalytic degradation of methylene blue (MB) were clarified. The mechanism provides a certain reference for the study of alkali metal doping modification of g-C_3N_4.

MATERIALS AND METHODS

Chemicals

Dicyandiamide was supplied by Tianjin Fuchen Chemical Reagent Factory, sodium chloride from Tianjin Tianli Chemical Reagent Co., Ltd., and MB from Tianjin Binhai Kedi Chemical Reagent Co., Ltd., China.

Preparation of g-C_3N_4 and Na^+-doped g-C_3N_4

Firstly, 4 g of dicyandiamide was dissolved in 30 ml of hot deionized water and slowly filled into 20 ml of NaCl solution under stirring. Then, the mixed solution was heated, concentrated, and dried at 60 °C. After that, it was ground and placed in a covered semi-closed crucible before placing in a muffle furnace. The heating rate was 2 °C/min, and the temperature was kept at 550 °C for 2 h. After natural cooling, the product was ground, impregnated with boiling water, dispersed by ultrasound, filtered, washed with hot water for many times, dried at 105 °C, and ground to obtain Na^+-doped g-C_3N_4 catalyst as Na(x)-CN, x refers to the molar concentration of NaCl in mol/l. If 20 ml of deionized water was used instead of 20 ml of NaCl solution; the other steps were the same as above, and g-C_3N_4 can be obtained.

Preparation of NaCl/g-C_3N_4 composite and g-C_3N_4 treated with NaCl solution

The prepared g-C_3N_4 was dispersed in 20 ml 0.1 mol/l NaCl solution, stirred, heated and concentrated, dried at 105 °C, and ground to obtain NaCl/g-C_3N_4 composite catalyst, which was denoted as CN@NaCl. After CN@NaCl was impregnated with boiling water, dispersed by ultrasound, filtered, washed with hot water for many times, dried and ground at 105 °C, the NaCl solution can be obtained to treat the g-C_3N_4 catalyst, which was denoted as CN/NaCl.

Photocatalyst characterization

The structure of catalyst was analyzed by X-ray diffractometer (XRD, Shimadzu XRD-7000) with Cu K_α (λ=0.15406 nm), the tube voltage is 40 kV, and the tube current is 30 mA). The morphology of catalyst was observed by scanning electron microscopy (SEM, Zeiss Sigma300) equipped with energy dispersive spectroscopy (EDS). The Na^+-doped amount in catalyst was confirmed using inductively coupled plasma mass spectrometry (ICP-MS, Perkin Elmer Elan6100DRC). The chemical composition and valence band position of catalyst were analyzed by X-ray photoelectron spectroscopy (XPS, Thermo Fisher, Escalab 250 Xi), and C 1s (284.8 eV) was used as the calibration peak for charge correction. The optical characteristics was carried out by UV-Vis diffuse reflectance spectrum (UV-Vis DRS, Shimadzu UV-2450) with $BaSO_4$ taken as reference material. The infrared spectra were recorded using Fourier transform infrared spectrometer (FTIR, Bruker Tensor 27) with wavenumber range from 4000 to 400 cm^{-1}. The pore size distribution, N_2 adsorption-desorption isotherm and specific surface area were analyzed by specific surface area and pore size analysis equipment (BET, Gold APP V-sorb 2800TP). The catalyst precursor was analyzed by thermogravimetric analyzer (TGA, Mettler-Toledo TGA/SDTA851) with N_2 (99.99%) flow rate 50 ml/min and temperature programmed from room temperature to 600 °C at 10 °C/min.

Photocatalytic activity measurements

The photocatalytic activities of these as-prepared photocatalysts were evaluated via degradation of MB under visible light irradiation. The 0.1 g of photocatalysts was added to 50 ml of 100 mg/l contaminant solution, followed by vigorous stirring for 1 h at room temperature in the dark. Subsequently, the degradation reaction was carried out under the light from a 400 W xenon lamp. The reaction solution was drawn at regular intervals and was filtered through a 0.45 μm microfiltration membrane. Finally, the diluted solution was used to determine the absorbance by UV-vis spectrometer at its characteristic peak of 664 nm.

RESULTS AND DISCUSSION

Characterization of photocatalysts

From Fig. 1, two characteristic diffraction peaks at 2θ = 13.0° and 27.3° appeared in the prepared catalysts, representing the (100) crystal plane of the g-C_3N_4 plane stacked graphite layer structure and the (002) crystal plane of the C-N aromatic heterocycle structure, respectively. In Fig. 1a, impurity diffraction peaks generated by incomplete decomposition and carbonization of dicyandiamide appeared at 2θ = 44.2°, 64.5° and 77.5°. Na^+-doped promoted the decomposition and carbonization of dicyandiamide. With the increase of Na^+-doped amount, the intensity of impurity diffraction peaks gradually decreased, while the intensity of catalyst characteristic diffraction peaks did not change significantly, and there was no characteristic peak related to Na species. In addition, the CN@NaCl catalyst exhibited characteristic peaks of NaCl at 2θ = 31.7°, 45.4° and 56.5°, while the diffraction peaks of CN/NaCl did not change (see Fig. 1b). Generally speaking, doping would change the lattice parameters of the original phase [26], but it was found from Fig. 1c that NaCl recombination, NaCl solution treatment or Na^+-doped did not change the diffraction peak position of the g-C_3N_4 (002) crystal plane. This finding may be due to the small radius of Na^+ so it would not destroy the crystal structure even if it enters the g-C_3N_4 crystal lattice. The doping amount of Na^+ in Na(0.04)-CN, Na(0.06)-CN, Na(0.08)-CN and Na(0.1)-CN was 0.49%, 0.73%, 1.1% and 1.36%, respectively, which was determined by ICP-MS. The results showed that the doping amount of Na^+ in Na(0.04)-CN, Na(0.06)-CN, Na(0.08)-CN and Na(0.1)-CN was 0.49 wt.%,

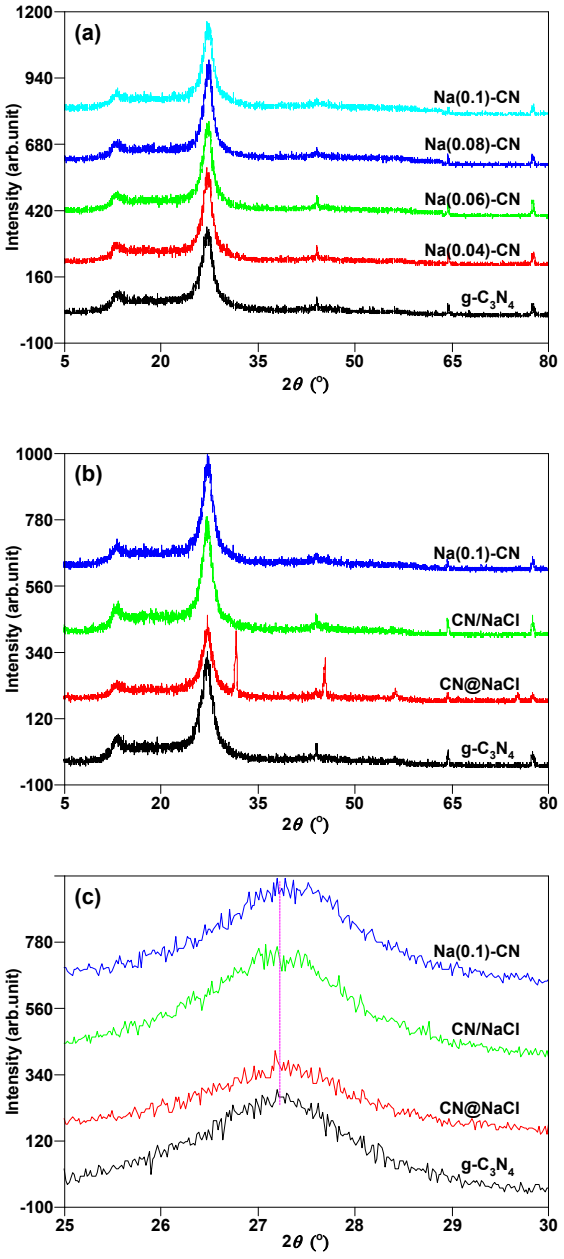

Fig. 1 XRD patterns of as-prepared catalysts.

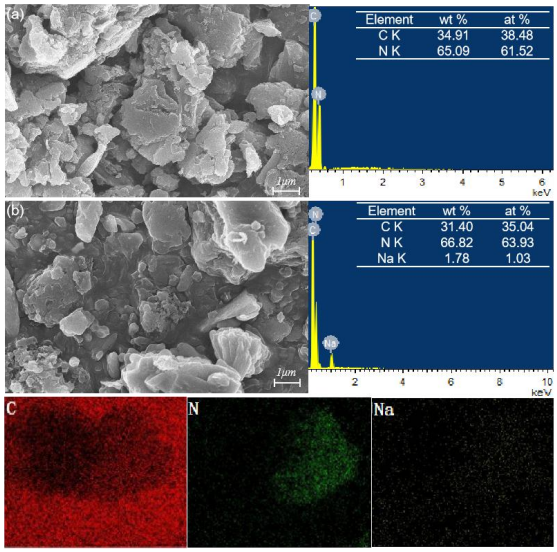

Fig. 2 SEM images and energy dispersive spectra of (a) g-C_3N_4 and (b) Na(0.1)-CN.

0.73 wt.%, 1.1 wt.% and 1.36 wt.%, respectively.

As shown in Fig. S1, all catalysts showed similar absorption peaks, which were basically consistent with XRD analysis results. The broad peaks between 3174–3435 cm^{-1} were the O-H stretching vibration peaks of water molecules in the catalyst and the N-H stretching vibration peaks of uncondensed amino groups on the surface. The peaks between 1242–1636 cm^{-1}, which were 1242, 1322, 1412, 1569 and 1636 cm^{-1} corresponded to the C-N and C=N stretching vibration peaks in C, N heterocyclic compounds. The absorption peak at 884 cm^{-1} corresponded to the N-H deformation peak, and 808 cm^{-1} was the characteristic peak of g-C_3N_4 heptazine structure. The existence of absorption peaks of 808 cm^{-1} and 1242–1636 cm^{-1} proved that all samples had a typical heptazine phase structure of g-C_3N_4. In addition, compared with other catalysts, Na(x)-CN had a stronger absorption peak at 2175 cm^{-1}, which is consistent with the position of azide framework vibration peak [27].

As displayed in Fig. 2, g-C_3N_4 presented an irregular layered structure with a large particle size, while Na(0.1)-CN had a large number of particles formed; the particle size was obviously smaller, and the combination between particles and layered structure was relatively close. In addition, C and N in g-C_3N_4 and C, N, and Na in Na(0.1)-CN were confirmed from energy dispersive spectra analysis. Moreover, the distribution of Na element in the whole measurement area was uniform, which indicated that doped Na^+ is uniformly dispersed in the crystal structure of g-C_3N_4.

As demonstrated in Fig. S2 and Table 1, both catalysts presented Type IV isotherms, indicating that both catalysts are mesoporous materials. The specific surface areas of g-C_3N_4 and Na(0.1)-CN calculated by BET method were 4.51 m^3/g and 5.53 m^3/g, respectively, which indicated that Na^+-doped reduces the particle size of the catalyst, increases the external special surface area (S_{ext}) and micropore special surface area (S_{mic}), and then results in an increase of the total specific surface area (S_{BET}) [28].

The light absorption properties of the catalysts have a significant impact on the photocatalytic perfor-

Table 1 Characteristics of g-C_3N_4 and Na(0.1)-CN.

Sample	S_{BET} (m^2/g)	S_{ext} (m^2/g)	S_{mic} (m^2/g)	d_m (nm)	Pore volume (cm^3/g)
g-C_3N_4	4.51	2.89	1.62	45.31	0.06
Na(0.1)-CN	5.53	3.70	1.83	31.87	0.04

S_{BET} (BET surface area) determined by BET model; S_{ext} (external surface area); S_{mic} (micropore surface area); d_m calculated by BJH method from desorption branch.

mance. As shown in Fig. S3a, the absorption boundary of g-C_3N_4 was 442 nm. With the increase of Na^+-doped amount, the absorbance of the catalyst increased, but the shift amplitude of the absorption boundary was small. As shown in Fig. S3b, the energy gap of g-C_3N_4, Na(0.04)-CN, Na(0.06)-CN, Na(0.08)-CN and Na(0.1)-CN are 2.68, 2.67, 2.66, 2.67 and 2.66 eV by the Kubelka-Munk equation, respectively. From Fig. S3c-d, it could be seen that the absorption boundaries and energy band widths of g-C_3N_4, Na(0.1)-CN, CN/NaCl and CN@NaCl were basically the same. This result showed that Na^+ modification had little effect on the optical properties of g-C_3N_4, which is different from other findings [29].

As displayed in Fig. S4a, the binding energies of the C 1*s* orbitals of g-C_3N_4 were located at 284.8 and 288.1 eV, corresponding to the C atom (C-N) in the graphite-like structure and the sp^2 hybrid C atom (N=C-N) in the cyclic structure, respectively. The N1s spectrum of g-C_3N_4 in Fig. S4b was divided into 3 peaks with binding energies at 398.4, 399.4 and 400.6 eV, belonging to the N atom of the sp^2 hybrid (C=N-C), the N atom in the 3-*s*-triazine ring (N–$(C)_3$) and the N atom in the terminal amino functional group (NH_2 and NH), respectively. Compared with g-C_3N_4, the binding energy of the C 1*s* orbital of Na(0.1)-CN was reduced by 0.2 eV, while the binding energy of the N 1*s* orbital was increased by 0.3–0.5 eV. As shown in Fig. S4c, the Na 1*s* orbital binding energy of Na(0.1)-CN was located at 1071 eV, which is 1 eV lower than that of NaCl (1072 eV), and basically coincides with that of NaN_3 (1070.8 eV) [28]. The results indicated that Na^+ exists in the lattice of g-C_3N_4 in the form of Na-N bond. The ionic radius of Na^+ is about 102 pm, which is much larger than the atomic radius of C and N (80–86 pm). In addition, g-C_3N_4 is a covalent compound, so Na^+ cannot be substituted and doped in the ionic state. It can only exist in the lattice gap of g-C_3N_4 in the form of Na-N bond. The higher electronegativity of N atom is used to balance the positive charge on Na^+ and improve the binding energy of the N 1*s* orbital of Na (0.1)-CN.

As depicted in Fig. S4d, Na^+-doped had a significant impact on the energy level position of the catalyst. The VB energy level position of g-C_3N_4 was 1.59 eV. After Na^+-doped generated Na(0.1)-CN, the VB energy level of the catalyst moved to the direction of high

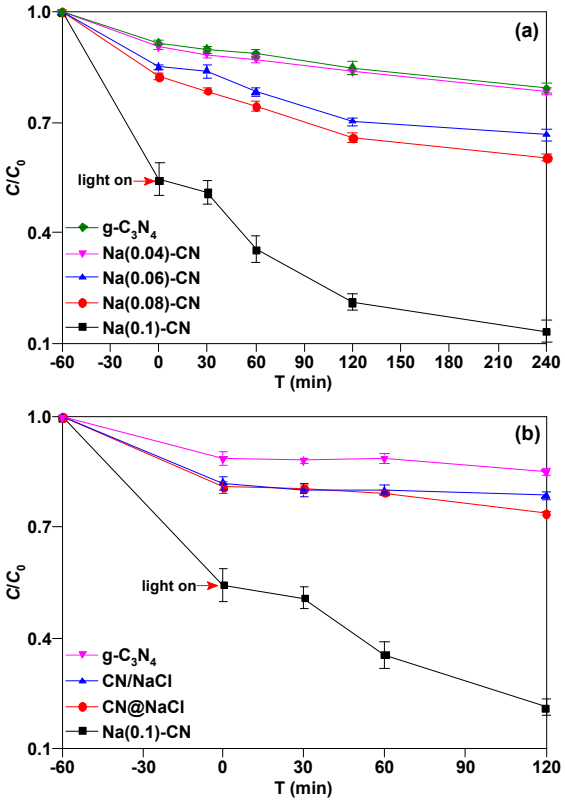

Fig. 3 Degradation curves of MB in visible light on different catalysts.

binding energy and was located at 1.68 eV. Combined with the test results of UV-Vis DRS, it is concluded that the CB energy level positions of g-C_3N_4 and Na(0.1)-CN were located at −1.09 and −0.98 eV, respectively, as shown in Fig. S5. The results showed that the energy band width of g-C_3N_4 could not be greatly changed by Na^+-doped, but the positions of VB and CB levels could be controlled.

As shown in Fig. 3a, before the xenon lamp was turned on, the removal rate of MB by g-C_3N_4 by adsorption was about 8.4%. With the increase of Na^+ doping amount, the removal rate gradually increased, and the removal rate of MB by Na(0.1)-CN was about 46%. When xenon lamp was turned on, Na(0.1)-CN showed the best photocatalytic performance, and the degradation rate of MB reached 87% after 240 min of illumination. Usually, the photocatalytic degradation reaction follows the first-order reaction kinetics: $-\ln(C/C_0) = kt$. Through fitting calculation, the rate constants k of g-C_3N_4, Na(0.04)-CN, Na(0.06)-CN, Na(0.08)-CN and Na(0.1)-CN were 0.0006, 0.0006, 0.0011, 0.0014 and 0.0063 min^{-1}, respectively. Na(0.1)-CN showed the maximum rate constant, which was about 10 times that of g-C_3N_4. As shown in Fig. 3b, the photocatalytic performance of g-C_3N_4 combined with NaCl or treated

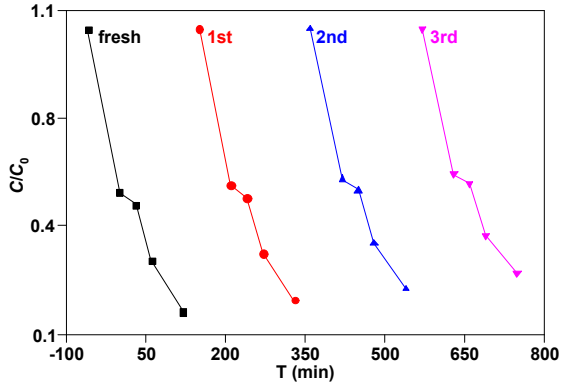

Fig. 4 Photocatalytic stability of Na(0.1)-CN.

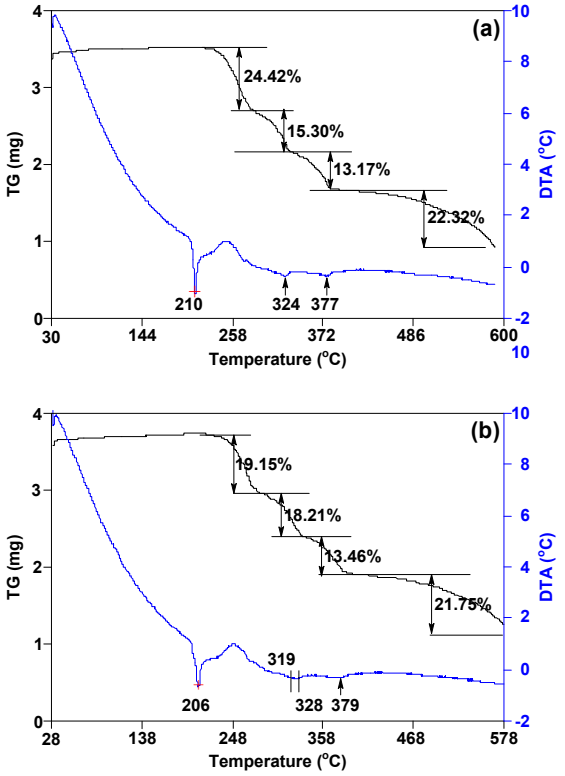

Fig. 5 TG-DTA curves of (a) g-C_3N_4 precursor and (b) Na(0.1)-CN precursor.

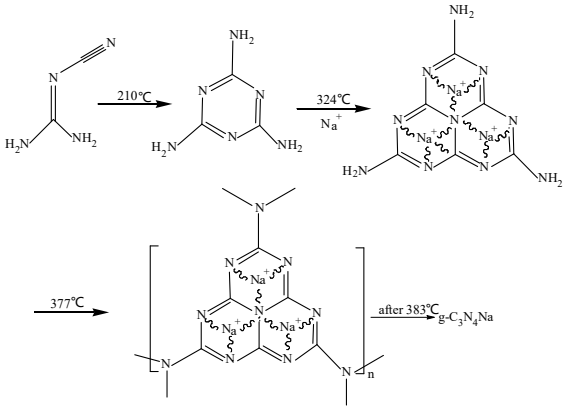

Fig. 6 Schematic diagram of Na(x)-CN synthesis mechanism.

with NaCl solution was not significantly improved. The morphology of the catalyst is regulated by Na^+-doped and generating Na-N bonds, so that the valence band position of the catalyst is significantly increased, which significantly improves the photocatalytic performance.

The photocatalytic stability test of Na(0.1)-CN was carried out and shown in Fig. 4. The results indicated that slight decrease in MB degradation performance was observed after 3 cycles. The ICP-MS result displayed that the Na concentration was 1.17 wt.% in Na(0.1)-CN which is very close to the fresh catalyst. Therefore, it is inferred that the chemical structure of Na(0.1)-CN is stable.

The precursors of g-C_3N_4 and Na(0.1)-CN were analyzed by TG-DTA. As shown in Fig. 5a, the process of dicyandiamide to produce g-C_3N_4 was divided into 4 stages, which is basically consistent with the literature report [30]. As depicted in Fig. 5b, the pyrolysis of dicyandiamide added with NaCl was still divided into 4 stages, and the temperature range of each stage was basically the same as that of Fig. 5a, but the weight loss rate of first stage decreased, which is related to the physical properties of NaCl that does not decompose and volatilize at low temperature. In the second stage, the weight loss rate increased, and a wide endothermic peak appeared at 319–328 °C. It is speculated that Na-N bond may be formed in this stage, which increases the deamination rate and ammonia production. According to the results of TG-DTA analysis, a schematic diagram of Na(x)-CN synthesis mechanism was drawn as shown in Fig. 6.

Based on the above analysis results, this paper puts forward assumptions on the mechanism of photocatalytic degradation of MB by Na(x)-CN as shown in Fig. 7. First, Na^+-doped generates Na-N bond, which reduces particle size of catalyst, increases specific surface area and micropore volume, and enhances its adsorption performance for dissolved oxygen and MB in water. Second, the surface of the catalyst is in a positively charged state due to Na^+-doped, which leads to the increase of the valence band position of Na(x)-CN and the enhancement of the oxidizability of holes (h^+).

CONCLUSION

When dicyandiamide and sodium chloride were co-heated to 319–328 °C, Na^+ was doped into the lattice gap of g-C_3N_4 in the form of Na-N bond. Na^+-doped

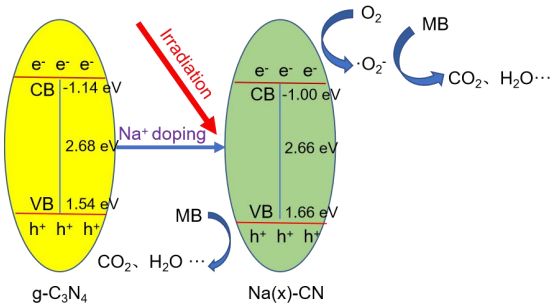

Fig. 7 Schematic diagram of the mechanism of photocatalytic degradation of MB by Na(x)-CN.

had little effect on the crystal structure and light absorption properties of g-C_3N_4, but the surface morphology of the catalyst changed from irregular layered structure to granular structure. The specific surface area and micropore volume increased, the valence band position increased, and the visible light catalytic performance was improved. Na(0.1)-CN had the best photocatalytic performance, and its degradation rate was about 10 times that of g-C_3N_4. The degradation rate of MB reached 87% after 4 h of illumination.

Appendix A. Supplementary data

Supplementary data associated with this article can be found at http://dx.doi.org/10.2306/scienceasia1513-1874.2022.046.

Acknowledgements: This work was supported by the National Natural Science Foundation of China (21663033).

REFERENCES

1. Somsongkul V, Chirawatkul P, Kongmark C (2021) Enhanced visible light response of TiO_2 nanoparticles by natural dyes. *ScienceAsia* **47S**, 69–75.
2. Li XB, Zhang HS, Luo JM, Feng ZJ, Huang JT (2017) Hydrothermal synthesized novel nanoporous g-C_3N_4/$MnTiO_3$ heterojunction with direct Z-scheme mechanism. *Electrochim Acta* **258**, 998–1007.
3. Li ZS, Lin RS, Liu ZS, Li DH, Wang HQ, Li QY (2016) Novel graphitic carbon nitride/graphite carbon/palladium nanocomposite as a high-performance electrocatalyst for the ethanol oxidation reaction. *Electrochim Acta* **191**, 606–615.
4. Bellardita M, García-López EI, Marcì G, Krivtsov I, García JR, Palmisano L (2018) Selective photocatalytic oxidation of aromatic alcohols in water by using P-doped g-C_3N_4. *Appl Catal B Environ* **220**, 222–233.
5. Fu JW, Zhu BC, Jiang CJ, Cheng B, You W, Yu JG (2017) Hierarchical porous O-doped g-C_3N_4 with enhanced photocatalytic CO_2 reduction activity. *Small* **13**, ID 1603938.
6. Zhu YX, Marianov A, Xu HM, Lang C, Jiang YJ (2018) Bimetallic Ag-Cu supported on graphitic carbon nitride nanotubes for improved visible-light photocatalytic hydrogen production. *ACS Appl Mater Inter* **10**, 9468–9477.
7. Li YD, Jiang YQ, Ruan ZH, Lin KF, Yu ZB, Zheng ZF, Xu XZ, Yuan Y (2017) Simulation-guided synthesis of graphitic carbon nitride beads with 3D interconnected and continuous meso/macropore channels for enhanced light absorption and photocatalytic performance. *J Mater Chem A* **5**, 21300–21312.
8. Zhang P, Li XH, Shao CL, Liu YC (2015) Hydrothermal synthesis of carbon-rich graphitic carbon nitride nanosheets for photoredox catalysis. *J Mater Chem A* **3**, 3281–3284.
9. She XJ, Liu L, Ji HY, Mo Z, Li YP, Huang LY, Du DL, Xu H, Li HM (2016) Template-free synthesis of 2D porous ultrathin nonmetal-doped g-C_3N_4 nanosheets with highly efficient photocatalytic H_2 evolution from water under visible light. *Appl Catal B Environ* **187**, 144–153.
10. Lan DH, Wang HT, Chen L, Au CT, Yin SF (2016) Phosphorous-modified bulk graphitic carbon nitride: Facile preparation and application as an acid-base bifunctional and efficient catalyst for CO_2 cycloaddition with epoxides. *Carbon* **100**, 81–89.
11. Liu H, Jin ZT, Xu ZZ, Zhang Z (2015) Fabrication of $ZnIn_2S_4$-g-C_3N_4 sheet-on-sheet nanocomposites for efficient visible-light photocatalytic H_2-evolution and degradation of organic pollutants. *RSC Adv* **5**, 97951–97961.
12. Bi LL, Xu DD, Zhang LJ, Lin YH, Wang DJ, Xie TF (2015) Metal Ni-loaded g-C_3N_4 for enhanced photocatalytic H_2 evolution activity: the change of surface band bending. *Phys Chem Chem Phys* **17**, 29899–29905.
13. Xu YG, Xu H, Wang L, Yan J, Li HM, Song YH, Huang LY, Cai GB (2013) The CNT modified white C_3N_4 composite photocatalyst with enhanced visible-light response photoactivity. *Dalton T* **42**, 7604–7613.
14. Zhang JS, Wang B, Wang XC (2014) Carbon nitride polymeric semiconductor for photocatalysis. *Prog Chem* **26**, 19–29.
15. Jin RR, You JG, Zhang Q, Liu D, Hu S, Gui JZ (2014) Preparation of Fe-doped graphitic carbon nitride with enhanced visible-light photocatalytic activity. *Acta Phys Chim Sin* **30**, 1706–1712.
16. Wang YG, Wang YZ, Chen YT, Yin CC, Zuo YH, Cui LF (2015) Synthesis of Ti-doped graphitic carbon nitride with improved photocatalytic activity under visible light. *Mater Lett* **139**, 70–72.
17. Yue B, Li QY, Iwai H, Kako T, Ye JH (2011) Hydrogen production using zinc-doped carbon nitride catalyst irradiated with visible light. *Sci Technol Adv Mat* **12**, ID 034401.
18. Rong XS, Qiu FX, Rong J, Zhu XL, Yan J, Yang DY (2016) Enhanced visible light photocatalytic activity of W-doped porous g-C_3N_4 and effect of H_2O_2. *Mater Lett* **164**, 127–131.
19. Le SK, Jiang TS, Zhao Q, Liu XF (2016) Cu-doped mesoporous graphitic carbon nitride for enhanced visible-light driven photocatalysis. *RSC Adv* **6**, 38811–38819.
20. Wang YG, Xu YL, Wang YZ, Qin HF, Li X, Zuo YH, Kang SF, Cui LF (2016) Synthesis of Mo-doped graphitic carbon nitride catalysts and their photocatalytic activity in the reduction of CO_2 with H_2O. *Catal Commun* **74**, 75–79.
21. Gao HL, Yan SC, Wang JJ, Huang YA, Wang P, Li ZS, Zou ZG (2013) Towards efficient solar hydrogen production by intercalated carbon nitride photocatalyst. *Phys Chem Chem Phys* **15**, 18077–18084.

22. Mohammad A, Khan ME, Yoon T, Cho MH (2020) Na,O-co-doped-graphitic-carbon nitride (Na,O-g-C_3N_4) for nonenzymatic electrochemical sensing of hydrogen peroxide. *Appl Surf Sci* **525**, ID 146353.
23. Li XW, Zhang HJ, Wen L, Dong F, Cen WL, Wu ZB (2016) *In-situ* synthesis, band structure analysis and of visible light photocatalysis enhancement mechanism of K-doped C_3N_4. *Chinese Sci Bull* **61**, 2707–2716.
24. Guo YR, Chen TX, Liu Q, Zhang ZG, Fang XM (2016) Insight into the enhanced photocatalytic activity of potassium and iodine codoped graphitic carbon nitride photocatalysts. *J Phys Chem C* **120**, 25328–25337.
25. Jiang J, Cao SW, Hu CL, Chen CH (2017) A comparison study of alkali metal-doped g-C_3N_4 for visible-light photocatalytic hydrogen evolution. *Chinese J Catal* **38**, 1981–1989.
26. Zhao JN, Ma L, Wang HY, Zhao YF, Zhang J, Hu SZ (2015) Novel band gap-tunable K-Na co-doped graphitic carbon nitride prepared by molten salt method. *Appl Surf Sci* **332**, 625–630.
27. Abedini R, Mosayebi A, Mokhtari M (2018) Improved CO_2 separation of azide cross-linked PMP mixed matrix membrane embedded by nano-CuBTC metal organic framework. *Process Saf Environ* **114**, 229–239.
28. Chen KL, Zhang SS, Yan JQ, Peng W, Lei DP, Huang JH (2019) Excellent visible light photocatalytic efficiency of Na and S co-doped g-C_3N_4 nanotubes for H_2 production and organic pollutant degradation. *Int J Hydrogen Energ* **44**, 31916–31929.
29. Fang WJ, Liu JY, Yu L, Jiang Z, Shangguan WF (2017) Novel (Na,O) co-doped g-C_3N_4 with simultaneously enhanced absorption and narrowed bandgap for highly efficient hydrogen evolution. *Appl Catal B Environ* **209**, 631–636.
30. Yang LR, Liu XY, Liu ZG, Wang CM, Liu G, Li QL, Feng XX (2018) Enhanced photocatalytic activity of g-C_3N_4 2D nanosheets through thermal exfoliation using dicyandiamide as precursor. *Ceram Int* **44**, 20613–20619.

Appendix A. Supplementary data

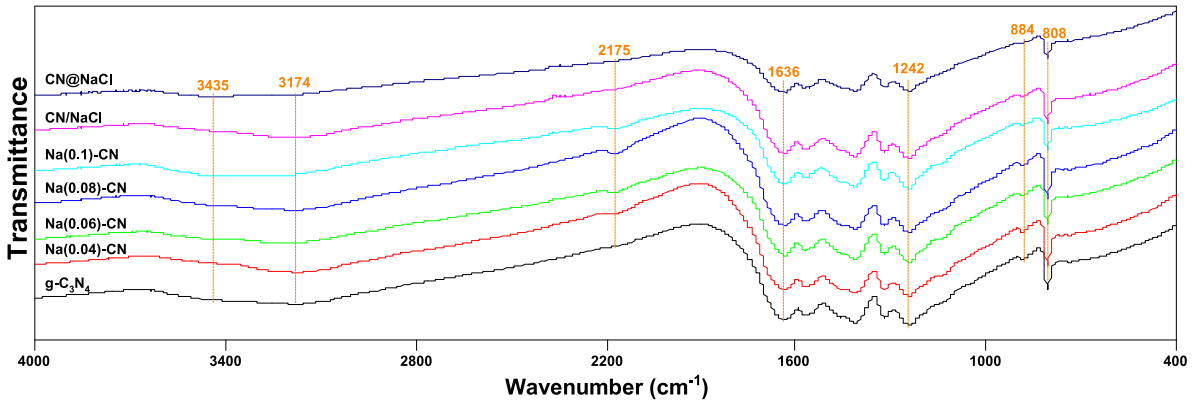

Fig. S1 FTIR spectra of as-prepared catalysts.

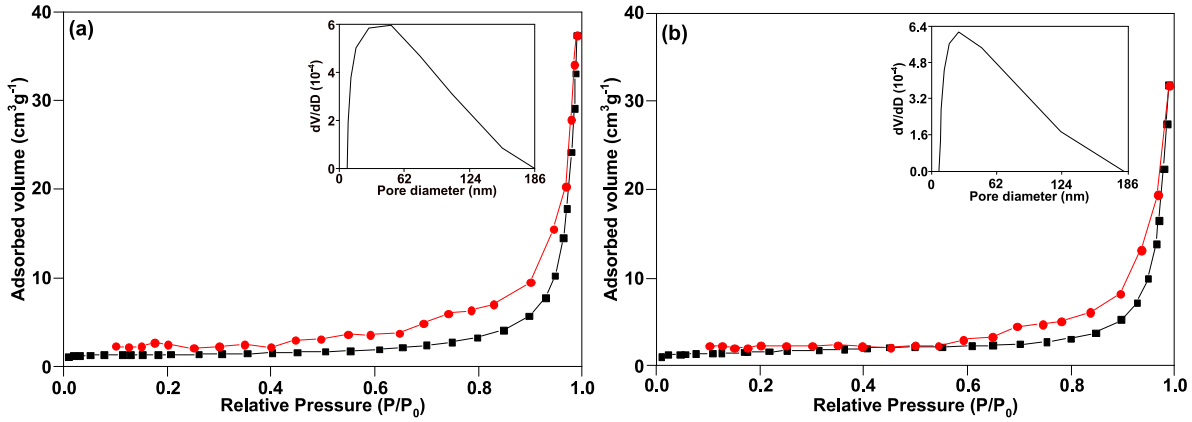

Fig. S2 N_2 adsorption-desorption isotherms of (a) g-C_3N_4 and (b) Na(0.1)-CN.

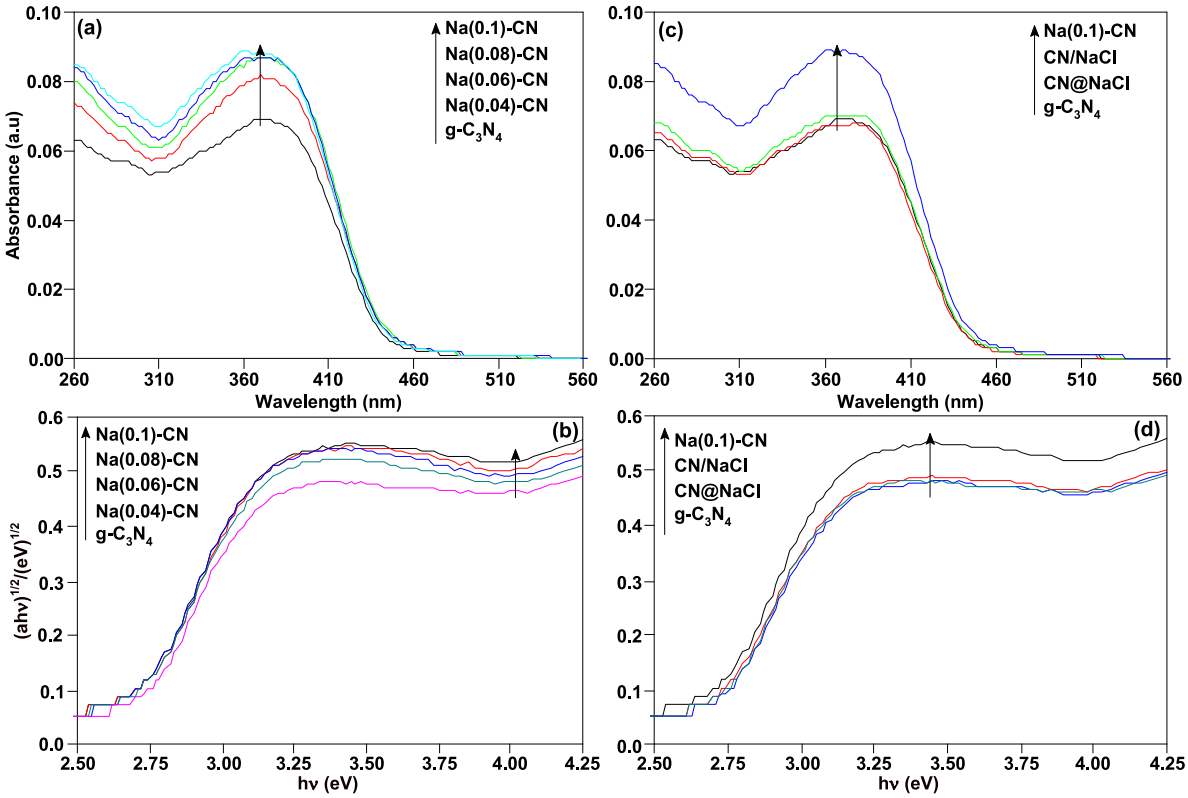

Fig. S3 (a) and (c) UV-Vis DRS spectra; (b) and (d) the plots of the $(\alpha h\nu)^{1/2}$ versus photon energy over the catalysts.

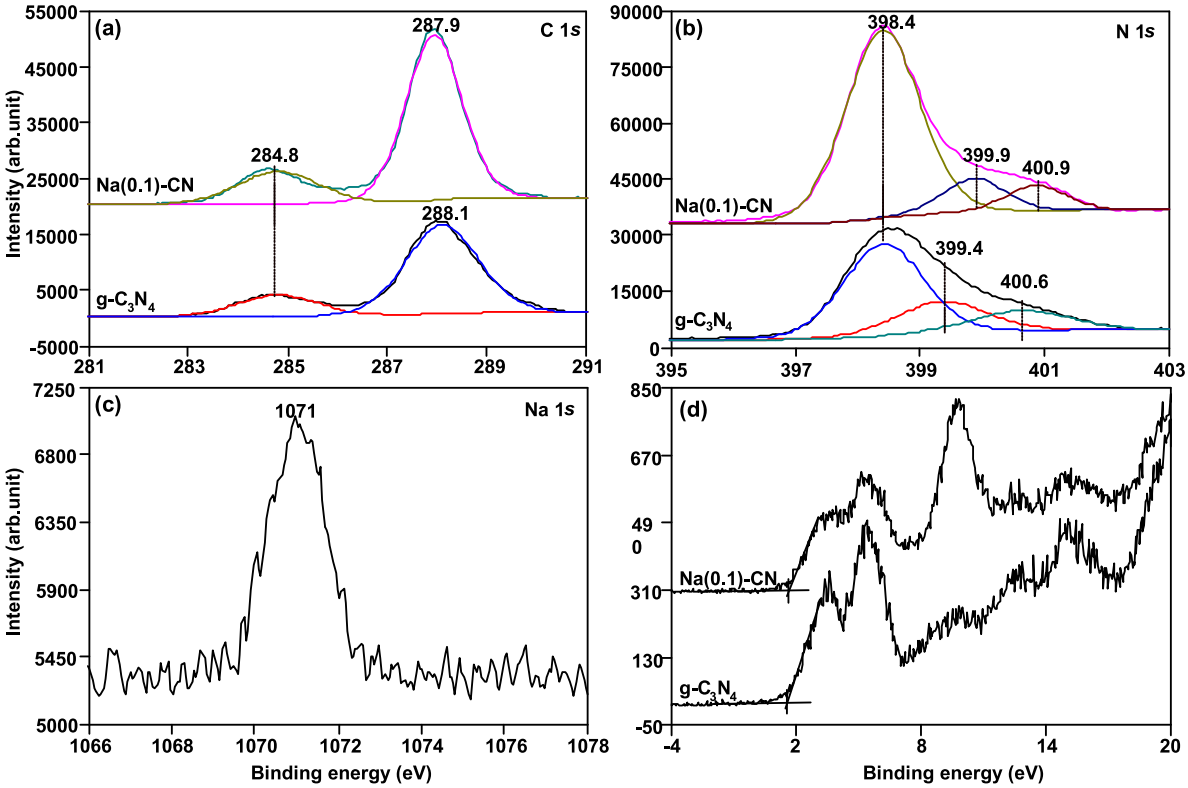

Fig. S4 XPS spectra of g-C_3N_4 and Na(0.1)-CN in the regions of (a) C 1*s*, (b) N 1*s*, (c) Na 1*s*, and (d) valence band.

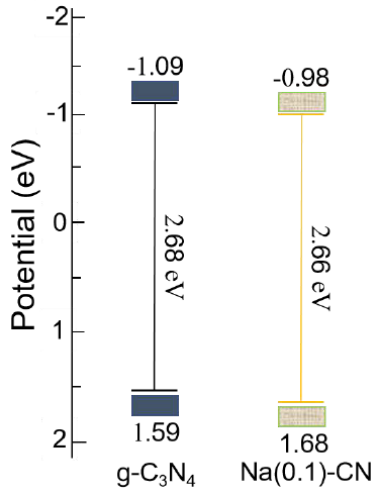

Fig. S5 Energy band structure of g-C_3N_4 and Na(0.1)-CN.